**JTAM (Jurnal Teori dan Aplikasi Matematika)**
http://journal.ummat.ac.id/index.php/jtam
p-ISSN 2597-7512 | e-ISSN 2614-1175
Vol. 9, No. 4, October 2025, pp. 1127-1141

# Assessing Solar Energy Potential through Sunshine Hour Interpolation using Spatiotemporal Kriging with Local Drift

**Salma Fitri Nugroho[1*], Rahma Fitriani[1], Atiek Iriany[1]**
[1]Department of Statistics, Universitas Brawijaya, Indonesia
salma_f@student.ub.ac.id

**Article History:**
Received : 07-06-2025
Revised : 26-06-2025
Accepted : 03-07-2025
Online : 01-10-2025

**Keywords:**
Interpolation;
Kriging;
Solar Energy;
Spatiotemporal;
Sunshine Hour.

**ABSTRACT**

Solar energy is a key renewable resource, particularly valuable in tropical regions like Bali, where sunlight is consistently available throughout the year. Accurate estimation of sunshine duration is essential for assessing solar energy potential, as it directly affects photovoltaic (PV) system performace and informs strategic planning for renewable energy development. This study aims to develop a spatiotemporal statistical interpolation model to estimate and predict sunshine duration patterns across Bali, thereby enhancing the planning and deployment of solar energy infrastructure. This quantitative research applies space-time kriging with local drift using sunshine duration data (in hours) collected from four meteorological stations between 2019 and 2023. The method effectively captures spatial and temporal dependencies by integrating local drift as a deterministic trend component. Among several models tested, the Gaussian-Gaussian-Gaussian (Gau-Gau-Gau) combination delivered the best performance, with an RMSE of 2.3085. The results show a clear seasonal cycle, with higher sunshine duration during the dry season (May–October) and lower values in the wet season (November–March). Northern and eastern Bali, particularly Buleleng and Karangasem, demonstrate the highest solar potential, while central mountainous areas show lower sunshine exposure due to cloud coverage. These results offer not only a methodological contribution through the application of spatiotemporal kriging with local drift, but also a practical framework for decision-makers. The insights can guide strategic placement of solar farms, optimize energy yield forecasts, and support resilient infrastructure planning in line with Bali's climatic realities and energy needs.

https://doi.org/10.31764/jtam.v9i4.32048



## A. INTRODUCTION

Solar energy has emerged as one of the most promising renewable energy sources worldwide, offering clean and sustainable alternatives to fossil fuels (Jaiswal et al., 2022). This transition is crucial as many countries face the dual challenges of growing electricity demand and worsening environmental degradation (Osman et al., 2023). Tropical regions, with high levels of solar irradiation are particularly well-positioned to benefit from solar energy technologies. As part of this global shift, Indonesia presents a strong case for solar energy development due to its equatorial position and consistent year-round solar exposure. Maximizing this potential requires a localized understanding of solar availability to guide infrastructure development and energy policy.

Indonesia has tropical climate and high solar radiation that offer significant potential for the solar energy development (Laksana et al., 2021). Within this national context, Bali Island stands

out with an average annual solar radiation of over 4.5 kWh/m$^2$/day (Pambudi et al., 2023). The island's relatively compact geography, reliable infrastructure and stable electricity demand that driven primarily by tourism and residential usage. It enhances its feasibility for solar-based energy solutions. However, despite its overall solar richness, Bali's geographical diversity introduces variation in solar energy potential. A strategic and spatially explicit assessment is therefore essential to support efficient planning and development of solar installations across the island.

The complex topography of Bali, from coastal lowlands to mountainous interiors like Mount Agung and Mount Batur significantly influences sunlight availability. Mountainous areas often experience orographic cloud formation, fog and localized rainfall which reduce sunshine hours. In contrast, lowland and coastal regions such as Denpasar and Sanur typically benefit from clearer skies and more sunshine exposure (Fitchett et al., 2025). These spatial disparities mean that generalized solar energy strategies may not be suitable. To ensure accurate planning, location-specific assessments are needed to quantify how terrain and climate affect sunshine duration which is a key factor in solar energy output.

Sunshine duration is the total hours of direct sunlight a location receives per day. It is a critical climatological parameter that influences photovoltaic (PV) performance (Bamisile et al., 2025). It plays a vital role not only energy planning (Kazaz & Istil, 2019) but also agricultural activities (Yuan et al., 2024), health (Sadiq et al., 2019), and overall daily human productivity (Zateroglu, 2021). In Bali, tourism and agriculture are highly dependent on weather conditions, understanding sunshine patterns is vital for both economic resilience and environmental planning. Despite its importance, sunshine duration data are typically collected at a limited number of meteorological stations, leading to sparse spatial coverage that restricts comprehensive regional analysis.

To address this limitation, advanced spatiotemporal interpolation methods such as kriging have been employed to estimate sunshine duration at unsampled locations. Space-time kriging with local drift is particularly effective, as it incorporates both spatial and temporal dependencies and accounts for external variables that influence the observed phenomenon. In the case of sunshine duration, these external variables often include seasonal effects driven by Bali's tropical climate. Previous studies Huang et al. (2024); Li et al. (2020); Dhaher & Shexo (2023) have demonstrated the utility of space-time kriging in environmental and meteorological data interpolation, emphasizing the need for models that handle non-stationarity and spatiotemporal variability. However, these models rarely consider seasonal components explicitly, especially in tropical regions like Bali.

This study addresses a significant research gap by integrating local drift derived from seasonal decomposition into the space-time kriging framework. Seasonal patterns, which cause systematic fluctuations in sunshine duration can violate the assumption of stationarity required by traditional kriging methods. By removing and separately modelling the seasonal component, the remaining data become more stationary and thus more suitable for space-time interpolation. This improvement allows for more accurate and realistic sunshine duration predictions across varying area.

This research aims to develop and apply a statistical interpolation model, specifically space-time kriging with local drift to estimate and predict sunshine duration across Bali using data

from 2019 to 2023. By producing high-resolution sunshine duration maps, this study aims to support optimal site selection for solar installations, improve energy yield forecasting, and guide strategic infrastructure planning aligned with Bali's environmental and economic needs.

## B. METHODS

### 1. Data and Research Variables

The data used in this study were obtained from the BMKG (*Badan Meteorologi, Klimatologi, dan Geofisika*) of Bali Province. The dataset consists of monthly average sunshine duration, a crucial variable for evaluating solar energy potential as it directly correlates with the amount of solar radiation that can be captured by photovoltaic (PV) systems. Data were collected from four observation stations across Bali; Denpasar area represented by Sanglah Geophysics Station, Jembrana area represented by Negara Climatology Station, Karangasem area represented by Kahang-Kahang Geophysics Station, and Badung area represented by Ngurah Rai Meteorology Station. These stations provide spatial coverage across urban, coastal, and inland areas, capturing diverse microclimates and geographical conditions.

Each station utilizes Campbell-Stokes sunshine recorders or automated solar radiation sensors, such as pyranometers, integrated into automatic weather stations (AWS), depending on the site's technological infrastructure. These instruments are standardized under World Meteorological Organization (WMO) guidelines to ensure consistent and reliable measurements of solar exposure. The observation period spans five years, from January 2019 to December 2023 with no missing data thus offering a robust and continuous temporal dataset for analysis. This temporal coverage allows for the examination of both interannual variability and seasonal trends in sunshine duration.

For analytical purposes, the sunshine duration data were structured into a space-time format using RStudio, which served as the primary software for data processing and statistical modeling. Sunshine duration, as a climatological variable, exhibits inherent variability over space and time. Therefore, the analysis proceeded in four key stages: (1) seasonal decomposition, (2) stationarity testing, (3) space-time semivariogram modeling, and (4) space-time kriging with local drift. The final results were visualized and mapped using ArcGIS, enabling the spatial interpretation of sunshine duration estimates across Bali.

### 2. Time Series Decomposition

The first step involved pre-processing the original time series data to ensure stationarity by removing seasonal component from each observation station through time series decomposition. Climatic data like sunshine duration generally exhibit strong seasonal fluctuations that make the data inherently non-stationary. Removing this seasonal trend improves the suitability of the data for further statistical analysis and modeling. The additive time series decomposition at each location was modeled and described mathematically as outlined in Equation (1) (Iftikhar et al., 2023).

$$Y(s,t) = Tr(s,t) + Se(s,t) + E(s,t) \quad (1)$$

where Y denotes the sunshine duration data in a space time context, measured at location *s* and time *t,* where *t* indicates the month ($t = 1, \dots, 12$). The variable Y consist of three components; $Tr$, representing the trend-cycle component; $Se$, the seasonal component; and $E$ is the irregular (random) component. In this study, only the seasonal component ($Se$) was removed, resulting seasonally adjusted data denoted as $R$ which modeled in Equation (2). This seasonal component is also referred to as local drift.

$$R(s,t) = Y(s,t) - Se(s,t) \quad (2)$$

### 3. Stationarity Checking using Regression Analysis

The second step of the analysis involved checking for stationarity using space-time regression model. Stationarity is a crucial assumption in this method, as non-stationary data can lead to misleading or biased result. This step ensures that any patterns or trends inherent in the data over space and time are appropriately accounted. The spatial trend variables are defined by the geographic coordinates longitude (x) and latitude (y) which represent the specific location of each observation point. Meanwhile the temporal trend is captured by the month in which each observation was recorded. This relationship is mathematically expressed in Equation (3)(Van Zoest et al., 2020).

$$R(s,t) = \sum_{i=0}^{p} \beta_i X_i(s,t) + \varepsilon_i(s,t) \quad (3)$$

where R refers to the seasonally adjusted dataset, which consists of $p + 1$ elements. The parameter $p$ signifies the number of independent variables included in the regression model. Specifically, this study using $p = 3$ represent longitude, latitude and month. The symbol $\beta_i$ indicates the regression coefficient for each variable, while $X_i(s,t)$ denotes the corresponding predictor variable defined over the space-time domain. More specifically, the expression $\beta_0 X_0(s,t)$ denotes the intercept term in the regression model. The subsequent terms account for the influence of the spatial and temporal variables on the response. Lastly, $\varepsilon_i(s,t)$ represents the residual term that not explained by the regression model.

### 4. Space-time Semivariogram

The third step is modeling these seasonally adjusted data using a space-time semivariogram, A space-time semivariogram characterizes both the spatial dependence of a regionalized variable and its temporal correlation over different time lags. There are two main types of space-time semivariograms used in this study, the empirical semivariogram which is derived from observed data, and the theoretical semivariogram which is fitted based on the empirical one. The empirical space time semivariogram provides a foundational understanding of the data structured and serves as the basis for fitting a theoretical model. The empirical semivariogram function is computed using Equation (4)(Medeiros et al., 2019).

$$\gamma_{st}(\boldsymbol{u}, \boldsymbol{v}) = \frac{1}{2} V(R(\boldsymbol{s} + \boldsymbol{u}, t + v) - R(\boldsymbol{s}, t)) \tag{4}$$

where, $u$ represents the spatial distance, while $v$ denotes the temporal lag. After constructing the empirical space-time semivariogram, the next step is to fit a theoretical semivariogram using an appropriate curve that best represents data. This fitting process involves comparing key components of the semivariogram such as the nugget effect, partial sill and range to determine the most suitable model.

In this study, the marginal semivariogram for both spatial and temporal dimensions are modeled using two different approaches using the combination of exponential and Gaussian model. These models are mathematically formulated in Equations (5) and (6), respectively.

$$\gamma(v) = c_0 + c\left[1 - \exp\left(-\frac{v}{a}\right)\right] \tag{5}$$

$$\gamma(v) = c_0 + c\left[1 - \exp\left(-\frac{v^2}{a^2}\right)\right] \tag{6}$$

where, $v$ refers the distance in either spatial or temporal term, $c_0$ denotes the nugget, $c$ represent the partial sill, and $a$ is an effective range.

After selecting appropriate semivariogram models for both spatial and temporal components, the next step is to construct the space-time semivariogram model that captures the structure of spatiotemporal dependence in the data. Several modeling approaches are available for this purpose, including the metric model, the separable model, the sum-metric model, and the sum-product model (Zhao et al., 2020; Lambardi Di San Miniato et al., 2022; O'Rourke & Kelly, 2015; Bachrudin et al., 2023).

In this research, the sum-metric model is chosen due to its greater flexibility in capturing the characteristics of the seasonally adjusted data (He et al., 2022). This model allows for the integration of both spatial and temporal components while maintaining a realistic representation of their interaction. The formulation of the sum-metric model is presented in Equation (7).

$$\gamma_{st}(\boldsymbol{u}, \boldsymbol{v}) = \gamma_{st}(\boldsymbol{u}, \boldsymbol{0}) + \gamma_{st}(\boldsymbol{0}, \boldsymbol{v}) + \gamma_{st}\sqrt{||u||^2 + (k.|v|)^2} \tag{7}$$

to determine the best model combination of spatial and temporal semivariogram model, a comparison will be conducted using the Root Mean Square Error (RMSE) as the evaluation metric shown in Equation (8) (Rahmawati, 2020).

$$RMSE = \sqrt{\frac{1}{\#N(\boldsymbol{u}, v)} \sum_{i=1}^{N(\boldsymbol{u},v)} \left(\hat{\gamma}(\boldsymbol{u}, v) - \gamma(\boldsymbol{u}, v)\right)^2} \tag{8}$$

A lower RMSE value indicates a better fit, as it reflects a smaller deviation between the modeled semivariogram and the empirical data. This comparison enables the selection of the

model that most accurately captures the underlying structure of the residuals.

### 5. Interpolation using Kriging with Local Drift

The final step is performing space-time local drift prediction of the data across all locations within the study area. The prediction is carried out using space-time kriging, which represent as Equation (9).

$$R^*(\boldsymbol{s_0}, t_0) = \sum_{i=1}^{n} \lambda_i \, R(\boldsymbol{s_i}, t_i) \tag{9}$$

where $R^*$ is the prediction value at unobserved location, $R$represent the seasonally adjusted value at the observed location, while $\lambda_i$ refers to the interpolation weights in the kriging process, as illustrated in Equation (10).

$$\begin{pmatrix} \gamma(\boldsymbol{s}_1 - \boldsymbol{s}_1, t_1 - t_1) & \cdots & \gamma(\boldsymbol{s}_1 - \boldsymbol{s}_n, t_1 - t_n) & 1 \\ \vdots & \ddots & \vdots & \vdots \\ \gamma(\boldsymbol{s}_n - \boldsymbol{s}_1, t_1 - t_1) & \cdots & \gamma(\boldsymbol{s}_n - \boldsymbol{s}_n, t_n - t_n) & 1 \\ 1 & \cdots & 1 & 0 \end{pmatrix} \begin{pmatrix} \lambda_1 \\ \vdots \\ \lambda_n \\ \alpha \end{pmatrix} = \begin{pmatrix} \gamma(\boldsymbol{s}_1 - \boldsymbol{s}_0, t_1 - t_0) \\ \vdots \\ \gamma(\boldsymbol{s}_n - \boldsymbol{s}_0, t_n - t_0) \\ 1 \end{pmatrix} \tag{10}$$

The space-time kriging with local drift estimation is given by Equation (11).

$$\hat{Z}_{(s_0,t_0)} = Se(s_0, t_0) + R^*(\boldsymbol{s_0}, t_0) \tag{11}$$

## C. RESULT AND DISCUSSION

### 1. Exploration

Figure 1 displays time series plots of monthly sunshine duration measured at four different stations located in Denpasar, Jembrana, Karangasem and Badung over the period from 2019 to 2023. Across all stations, a strong seasonal pattern is evident with sunshine duration increasing during the dry season in May to October and decreasing during the wet season in November to March. This cyclical trend aligns with Bali's climate which features clearly defined wet and dry periods, as shown in Figure 1.

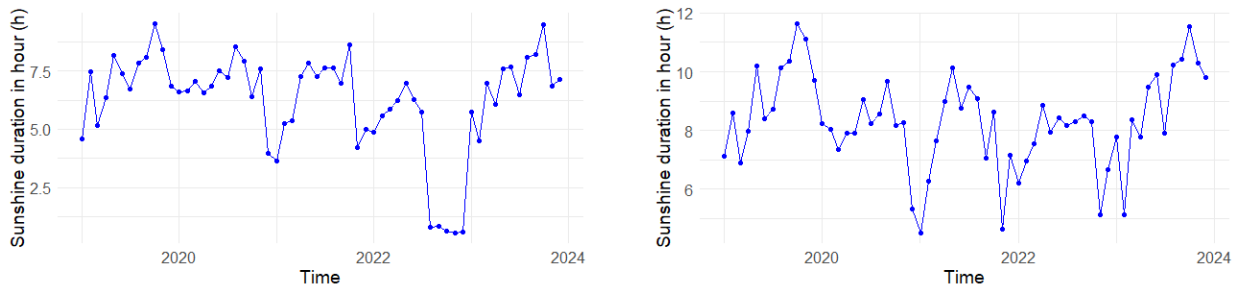


(a) (b)

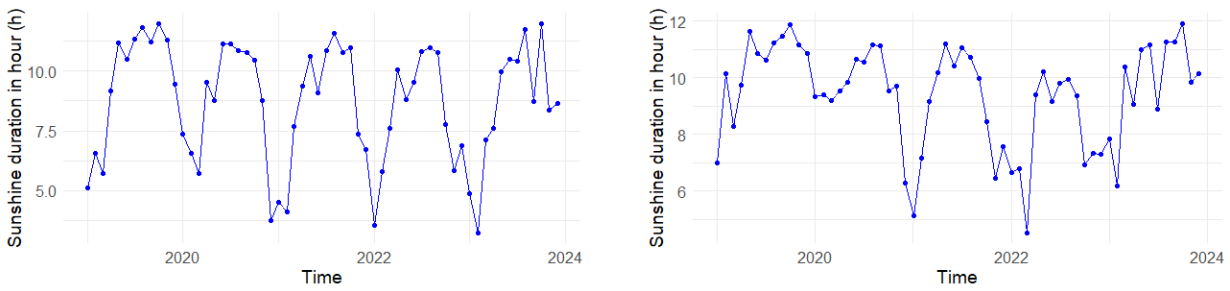


(c) (d)

**Figure 1.** Time series plot at (a) Sanglah Geophysics Station, (b) Negara Climatology Station, (c) Kahang-Kahang Geophysics Station, and (d) Ngurah Rai Meteorology Station

From the Figure 1, there is a clear cyclical pattern in Sanglah station with generally increases around mid-year while dry season and decreasing during the wet season around early and late months of the year. The fluctuations are relatively smoother compared to other stations. This is posibly due to urban influences or coastal proximity. A seasonal pattern is also evident at the Negara station, although it exhibit slightly greater fluctuations compared to Sanglah station. Sunshine duration tends to decreases significantly during the rainy months and consistently recovers during the dry season. It may be influenced by local topography or heavier rainfall.

Kahang-Kahang station exhibits the most pronounced seasonal fluctuations. There are sharp and consistent peaks during the dry season and steep declines throughout the wet season. This is likely due to its mountainous or inland location that tends to amplify seasonal contrast. The variation in Ngurah Rai station is not as extreme as in Kahang-Kahang, with the peaks around the mid-year and lower values at the beginning and end. It possibly influenced by its coastal location near the airport.

Overall, a seasonal pattern is clearly visible in all four locations, characterized by recurring peaks and troughs that appear every 12 months. This pattern indicates the presence of strong annual cycles reflected the region's well-defined dry and wet seasons, which are typical of Bali's tropical climate. The regular seasonal fluctuations highlight the need for time series decomposition to remove the seasonal components prior to conducting further space-time modeling. This preprocessing step is crucial to ensure the stationarity assumption required for reliable space-time kriging analysis in the subsequent stages.

## 2. Time Series Decomposition

To address the strong seasonality in sunshine duration, a time series decomposition was applied separately to each observation station. The additive decomposition technique was employed to separate the observed data into trend, seasonal, and residual components. This method is suitable when the magnitude of seasonal variation remains consistent over time. Figure 2 presents the results of this decomposition for the four meteorological stations in Bali, based on Equation (1).

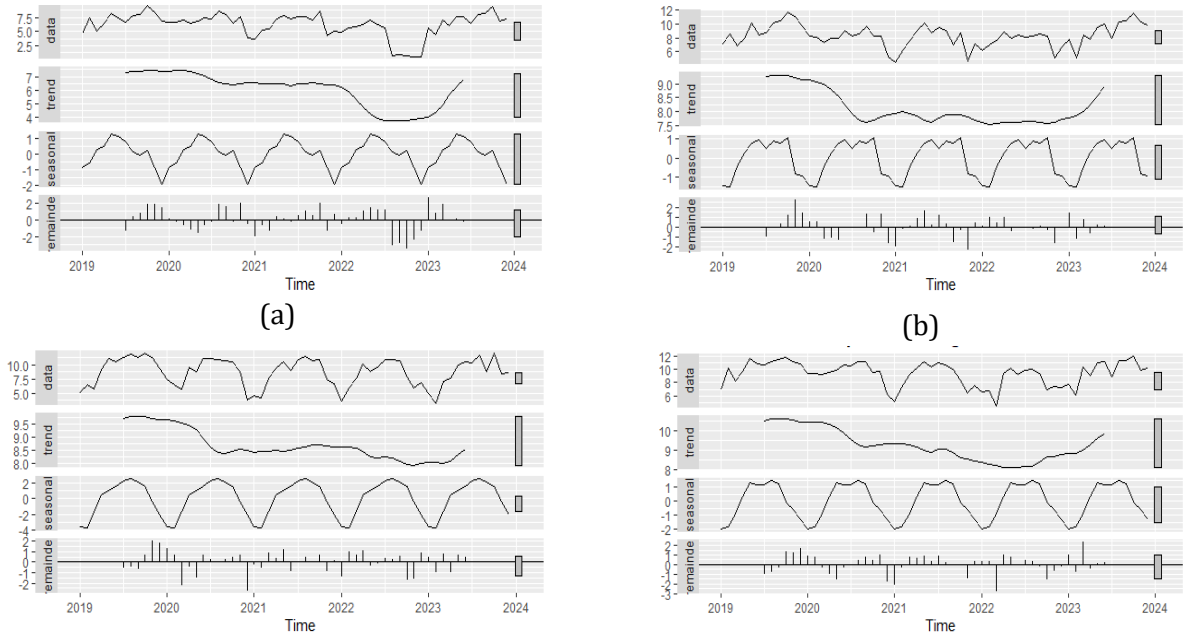


**Figure 2.** Decomposition plot at (a) Sanglah Geophysics Station, (b) Negara Climatology Station, (c) Kahang-Kahang Geophysics Station, and (d) Ngurah Rai Meteorology Station

From Figure 2, a clear seasonal cycle is observed at Sanglah Geophysics Station. Sunshine duration typically reached the highest point between April and August, inline to Bali's dry season. Furthermore, align with the peak of wet season, sunshine duration dips around December and February. The trend remains relatively stable after 2022 indicates consistent climatic patterns in this region. Similarly, Negara Climatology Station in Jembrana also exhibits a regular seasonal pattern where the sunshine duration increases in the middle year and decreases toward the end of the year. The residuals suggest some noise but no major shift in the overall trend.

In contrast, Kahang-Kahang Geophysics Station in Karangasem displays a stronger seasonal fluctuation, implying greater variation between dry and wet seasons in East Bali. The amplitude of the seasonal component is larger compared to other stations. It indicates more extreme seasonality in this area. This region experiences more extreme transitions in sunshine duration throughout the year. A comparable pattern is observed at Ngurah Rai Meteorology Station in Badung, where seasonal variation is also evident. The relatively small residuals across stations suggest that these seasonal behaviours are stable and predictable. Overall, the findings reflect typical Bali's tropical climate where the sunshine duration is highest during the dry season that occur between April to September and consistently lower during the wet season between November until March. The specific deviation of seasonal component that called as a local drift are shown in Tabel 1.

**Table 1.** Seasonal deviation at each observed station as a local drift

| | Jan | Feb | Mar | Apr | May | Jun | Jul | Aug | Sep | Oct | Nov | Dec |
|---|---|---|---|---|---|---|---|---|---|---|---|---|
| Sanglah | -0.84 | -0.56 | 0.262 | 0.472 | 1.279 | 1.156 | 0.752 | 0.146 | -0.09 | 0.238 | -0.86 | -1.95 |
| Negara | -1.46 | -1.53 | -0.40 | 0.254 | 0.750 | 0.927 | 0.485 | 0.876 | 0.785 | 1.064 | -0.83 | -0.92 |
| Kahang-Kahang | -3.64 | -3.77 | -1.62 | 0.505 | 0.948 | 1.501 | 2.240 | 2.545 | 2.146 | 1.550 | -0.39 | -2.01 |
| Ngurah Rai | -2.01 | -1.84 | -0.91 | 0.323 | 1.345 | 1.148 | 1.190 | 1.485 | 1.216 | -0.08 | -0.59 | -1.26 |

Kahang-Kahang Station exhibits the most pronounced seasonal variation in sunshine duration with the largest local drift range. This indicates significant differences between the wet and dry seasons. It likely due to its inland or elevated topography, which tends to intensify seasonal contrasts. In comparison, Sanglah and Ngurah Rai stations also show distinct seasonal cycles, but with more moderate fluctuations. It suggests a less extreme difference between seasons. Among the four stations, Negara Station displays the least seasonal variation indicates a relatively stable pattern of sunshine duration throughout the year. This steadiness may be attributed to its coastal location.

Overall, sunshine duration across Bali is closely tied to the Bali's tropical climate. All observation stations experience a clear decreased in sunshine duration during the wet season around November to March and increased during the dry season around May to October. The seasonal deviation that detailed in Table 1 will be removed from the original data based on Equation (2). This step is essential, as seasonal variation violates the underlying assumptions of space-time kriging which requires stationarity. The resulting dataset with the local drift is referred to as seasonally adjusted data.

## 3. Stationarity Checking using Regression Analysis

Stationarity is a critical assumption in kriging, as the method requires that statistical properties such as mean and variance remain constant over space and time. If the seasonally adjusted sunshine duration data still contains underlying trends, it may bias the interpolation results. To verify stationarity, a regression analysis was performed using sunshine duration as the response variable and time, latitude, and longitude as explanatory variables. The results are summarized in Table 2.

**Table 2.** Result of regression analysis

| Parameter | Parameter Estimation | t test | | $R^2$ | F test |
|---|---|---|---|---|---|
| | | t value | p-value | | p-value |
| $\beta_0$ (intercept) | -13.0829 | -0.328 | 0.7434 | 0.0174 | 0.2463 |
| $\beta_1$ (longitude) | 0.2684 | 0.766 | 0.4443 | | |
| $\beta_2$ (latitude) | 1.1570 | 1.685 | 0.0934 | | |
| $\beta_3$ (time) | 0.0364 | 1.026 | 0.3059 | | |

The regression analysis presented in Table 2 confirms that after removing seasonal components, the sunshine duration data achieves a stationary state across both space and time. This is shown by the non-significant p-values in the t-test for all regression parameter. Additionally, the overall model is not statistically significant since the p-value is well above the alpha of 0.05. These findings indicate there are no meaningful trend.

From a geographical perspective, sunshine duration in northeast area like Karangasem, might be slightly higher due to clearer skies in mountainous areas. It aligns with the higher latitude coefficient, although it is not significant. Conversely, urban and coastal area such as Denpasar and Badung often experience more stable sunshine duration patterns. This is might be influenced by urban microclimates and coastal haze which can diffuse or reduce sunshine intensity. These microclimatic factors may explain the weak spatial dependence observed in the regression model. Temporally, the absence of a significant trend over the five-year period implies that sunshine duration patterns remained relatively stable. This reinforces the assumption of a consistent climatic background across the study period, further validating the use of kriging techniques on the seasonally adjusted dataset.

## 4. Space-time Semivariogram

The space-time semivariogram provides insight into the structure of spatial and temporal dependence in sunshine duration across Bali. By quantifying how similarity diminishes with increasing spatial and temporal separation, it supports the selection of an appropriate theoretical model for interpolation. The empirical semivariogram, computed using Equation (4), is presented in Figure 3.

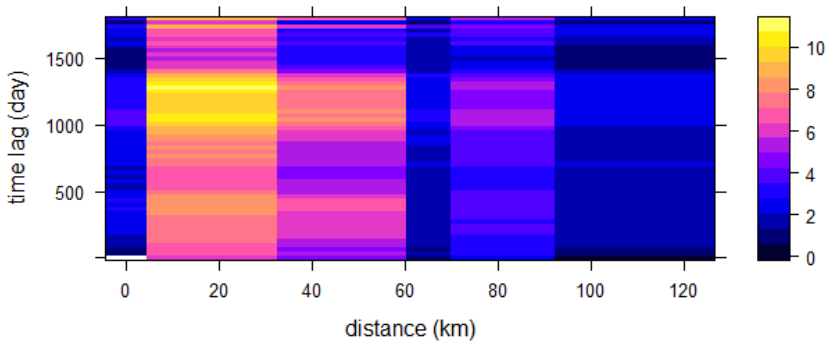


**Figure 3.** Empirical semivariogram

From the Figure 3, at short spatial distances less than 40 km, semivariance remains low to moderate that indicate a strong spatiotemporal autocorrelation. In practical terms, this means that sunshine duration at nearby locations tends to be similar in over shorter time lag. However, a notable increase in semivariance is observed between 40 and 60 km indicates the existence of a spatial decorrelation zone. This marks a transition zone where sunshine duration begins to diverge more significantly between locations.

On the temporal terms, semivariance gradually increases beyond time lag of approximately 1,000 days, even when spatial distance is small. This trend reflects a typical temporal decay in autocorrelation for climatic variables where weather conditions diverge over multi-year timescales. However, the relatively moderate increase in semivariance suggests that Bali's sunshine duration remains fairly stable over time. The performance of various space-time semivariogram model combinations, evaluated through Root Mean Square Error (RMSE) presented in Table 3. It is supporting the selection of the best-fitting theoretical model for sunshine duration estimation.

**Table 3.** Comparison of RMSE for fitting theoretical semivariogram model

| Joint Model | Space-time Combination Model | | | |
|---|---|---|---|---|
| | **Exp-Exp** | **Exp-Gau** | **Gau-Exp** | **Gau-Gau** |
| Exp | 2.308536 | 2.308537 | 2.308536 | 2.308537 |
| Gau | 2.308497 | 2.308496 | 2.308497 | 2.308496 |

Table 3 presents the Root Mean Square Error (RMSE) values for several theoretical space-time semivariogram models fitted to the empirical sunshine duration data. Among the six joint model combinations evaluated, the Gaussian-Gaussian-Gaussian (Gau-Gau-Gau) model produced the lowest RMSE value of 2.308496. It offers the best fit of the observed spatiotemporal variability. This result suggests that the Gau-Gau-Gau model most effectively captures the underlying structure of sunshine duration across both space and time in Bali. The fitted space-time semivariogram based on the best-performing model is illustrated in Figure 4.

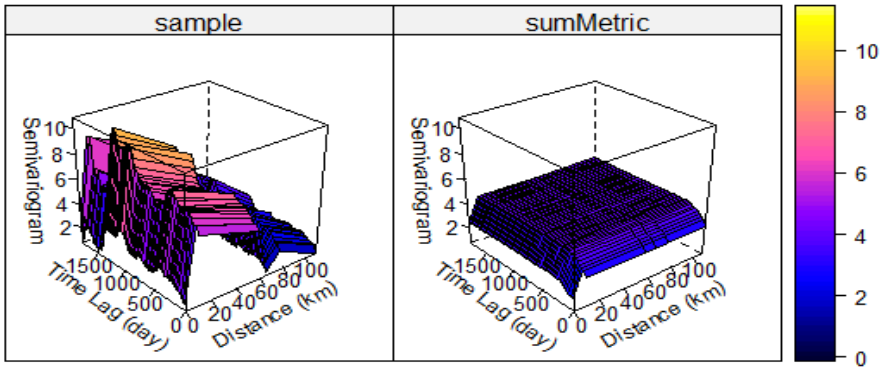


**Figure 4.** Space-time semivariogram

The left side of Figure 4 presents the empirical semivariogram which characterized by irregular fluctuations and sharp peaks across the surface. These variations indicate a strong interaction between spatial and temporal component in sunshine duration. Moreover, the theoretical space-time semivariogram shown on the right side is derived using Gau-Gau-Gau sum-metric model. This plot shows a smoother and more continuous surface reflecting the fitted values obtained from the selected theoretical model.

In this model, the joint space-time component is represented by Gaussian model which contributes a partial sill of 0.8936 and a range of 10.000,34. This high range reflects the gradual decay in correlation typical of climatic variables such as sunshine duration. The model also estimates a space-time anisotropy (stAni) of approximately 65.85 means that one month increase is equivalent to a 65.85 km change in spatial distance. This anisotropy underscores the interconnectedness of space and time in driving sunshine variability across Bali where temporal changes often mirror spatial transitions, particularly between lowland and highland regions or across wet and dry seasons. Overall, the low RMSE value and strong visual alignment between the empirical and theoretical semivariograms validate the use of the Gau-Gau-Gau model. This model provides a reliable foundation for subsequent space-time kriging and high-resolution sunshine duration prediction.

## 5. Space-Time Kriging with Local Drift

In the final modelling step, the previously removed seasonal component was reintroduced to each predicted point by referencing the nearest observation station. This adjustment ensures that the final sunshine duration estimates reflect both the localized seasonal behavior (local drift) and the residual variability captured by space-time kriging. The final sunshine duration predictions, which incorporate both the local drift and the adjusted kriging values, are illustrated in Figure 5.

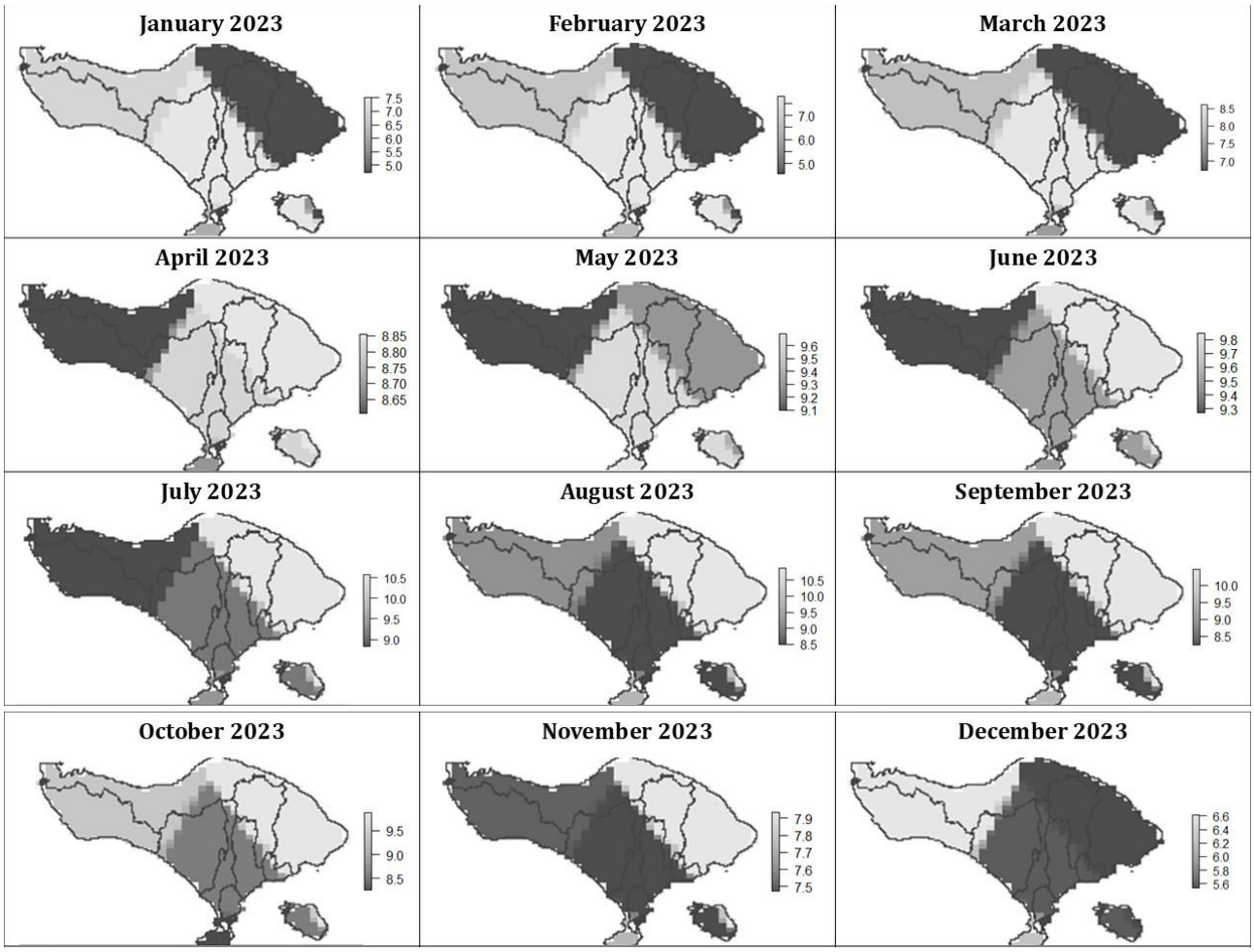


**Figure 5.** Sunshine duration prediction map using space-time kriging with local drift

Figure 5 present the monthly spatial predictions of sunshine duration across Bali for the year 2023 using space-time kriging with local drift. This figure provides valuable insight into the island's solar energy potential as sunshine duration is a key factor influencing photovoltaic (PV) system performance. Regions with consistently high sunshine hours offer optimal conditions for solar power generation, while regions with low duration may require alternative energy strategies.

Regionally, northern Bali (e.g., Buleleng, parts of Karangasem) consistently records the highest sunshine duration that often exceeding 9 hours/day especially between May and September. It happened due to its relatively dry area, inland conditions and lower cloud density. This makes it highly suitable for utility-scale solar farms. Eastern Bali, particularly Karangasem

shows high solar potential with strong seasonal variation. The combination of lower population density and topographic diversity provides good opportunities for targeted solar development.

Western Bali (Jembrana and Negara) experiences moderate sunshine throughout the year with slightly lower than the north and east. The influence of coastal moisture may explain the marginally reduced values. In southern Bali, including Denpasar, Badung, Sanur and Nusa Dua, sunshine duration more stable yet relatively lower in the wet season. Urban haze, coastal humidity and air pollution may reduce solar efficiency. While in central Bali like Bangli and areas near Mt. Batur and Mt. Agung, records the lowest sunshine duration across the year. The high elevation and mountainous terrain cause frequently cloud cover and afternoon rainfall that significantly limiting solar exposure. However, hybrid energy systems may offer a more reliable solution for sustainable energy development.

Overall, the predicted sunshine duration maps reflect the distinct seasonal rhythm of Bali's tropical climate. Sunshine duration increases during the dry season around April to October, peaking in August and September. While the wet season in November to March shows markedly reduced sunshine duration due to increased cloud cover and precipitation. Align with the study by Hasibuan et al. (2024), this seasonal fluctuation indicates that solar energy systems in Bali would perform most efficiently during the dry months, with reduced output expected during the rainy season. These insights provide essential guidance for planning solar infrastructure and optimizing energy yield across different regions of the island.

## D. CONCLUSION AND SUGGESTIONS

This study aimed to analyse and predict sunshine duration across Bali Island using space-time kriging with local drift. The findings demonstrate that this method effectively captures both the seasonal dynamics and spatial variability of sunshine duration, offering a statistically robust framework for spatiotemporal interpolation in tropical regions. Among the six model combinations evaluated, the Gaussian-Gaussian-Gaussian (Gau-Gau-Gau) model achieved the best performance, with the lowest RMSE value of 2.3085. The resulting predictions align with Bali's well-known monsoonal climate, showing longer sunshine durations during the dry season around May to October and shorter durations during the wet season around November to March. Importantly, the results confirm that sunshine duration is not uniformly distributed across the island, with variations influenced by topography, proximity to the coast, and local microclimatic factors. The main contribution of this research lies in its integration of seasonal components as local drift into the space-time kriging framework, which enhances model accuracy by addressing the non-stationarity commonly found in climatic data. This approach provides a refined estimation of sunshine duration, making it especially valuable for renewable energy studies in tropical regions like Bali. The model outputs offer practical insights for decision-makers involved in solar energy planning, such as identifying priority areas for solar farm development, optimizing energy yield forecasts, and guiding infrastructure investment based on regional sunshine potential. Additionally, the results support sustainable tourism and land-use strategies by enabling more climate-resilient planning. To further improve model performance and generalizability, it is recommended to expand the dataset by incorporating a longer temporal span and increasing the number of observation stations, particularly in currently underrepresented inland and mountainous areas. These enhancements will not only

improve the spatial resolution and predictive accuracy of the model but also ensure more comprehensive coverage of Bali's diverse geographic and climatic conditions, thereby supporting more inclusive and data-driven energy development strategies.

**ACKNOWLEDGEMENT**

The author gratefully acknowledges the supervisors and reviewers for their valuable contributions and insightful feedback, which have significantly enhanced the quality of this research.

**REFERENCES**

Bachrudin, A., Ruchjana, B. N., Abdullah, A. S., & Budiarto, R. (2023). Spatio-Temporal Model of a Product–Sum Simulation on Stream Network Based on Hydrologic Distance. *Water*, *15*(11), 2039. https://doi.org/10.3390/w15112039

Bamisile, O., Acen, C., Cai, D., Huang, Q., & Staffell, I. (2025). The environmental factors affecting solar photovoltaic output. *Renewable and Sustainable Energy Reviews*, *208*(1), 115073. https://doi.org/10.1016/j.rser.2024.115073

Dhaher, G., & Shexo, A. (2023). Using Kriging Technique to Interpolate and Forecasting Temperatures Spatio-Temporal Data. *European Journal of Pure and Applied Mathematics*, *16*(1), 373–385. https://doi.org/10.29020/nybg.ejpam.v16i1.4613

Fitchett, J. M., Roffe, S. J., & Prinsloo, A. S. (2025). Evaluating sunshine hour approximation for biometeorological indices. *Theoretical and Applied Climatology*, *156*(1), 13. https://doi.org/10.1007/s00704-024-05237-6

Hasibuan, A., Nrartha, I. M. A., Fithra, H., Desky, M. A., Isa, M., Siregar, W. V., Nurdin, N., & Kurniawan, R. (2024). Rainy and dry seasons impact on electricity demand in Indonesia. *SINERGI*, *28*(3), 545. https://doi.org/10.22441/sinergi.2024.3.011

He, Q., Zhang, K., Wu, S., Lian, D., Li, L., Shen, Z., Wan, M., Li, L., Wang, R., Fu, E., & Gao, B. (2022). An investigation of atmospheric temperature and pressure using an improved spatio-temporal Kriging model for sensing GNSS-derived precipitable water vapor. *Spatial Statistics*, *51*, 100664. https://doi.org/10.1016/j.spasta.2022.100664

Huang, J., Lu, C., Huang, D., Qin, Y., Xin, F., & Sheng, H. (2024). A Spatial Interpolation Method for Meteorological Data Based on a Hybrid Kriging and Machine Learning Approach. *International Journal of Climatology*, *44*(15), 5371–5380. https://doi.org/10.1002/joc.8641

Iftikhar, H., Bibi, N., Canas Rodrigues, P., & López-Gonzales, J. L. (2023). Multiple Novel Decomposition Techniques for Time Series Forecasting: Application to Monthly Forecasting of Electricity Consumption in Pakistan. *Energies*, *16*(6), 2579. https://doi.org/10.3390/en16062579

Jaiswal, K. K., Chowdhury, C. R., Yadav, D., Verma, R., Dutta, S., Jaiswal, K. S., SangmeshB, & Karuppasamy, K. S. K. (2022). Renewable and sustainable clean energy development and impact on social, economic, and environmental health. *Energy Nexus*, *7*(1), 100118. https://doi.org/10.1016/j.nexus.2022.100118

Kazaz, A., & Adiguzel Istil, S. (2019). A Comparative Analysis of Sunshine Duration Effects in terms of Renewable Energy Production Rates on The LEED BD + C Projects in Turkey. *Energies*, *12*(6), 1116. https://doi.org/10.3390/en12061116

Laksana, E. P., Prabowo, Y., Sujono, S., Sirait, R., Fath, N., Priyadi, A., & Purnomo, M. H. (2021). Potential Usage of Solar Energy as a Renewable Energy Source in Petukangan Utara, South Jakarta. *Jurnal Rekayasa Elektrika*, *17*(4), 212–216. https://doi.org/10.17529/jre.v17i4.22538

Lambardi Di San Miniato, M., Bellio, R., Grassetti, L., & Vidoni, P. (2022). Separable spatio-temporal kriging for fast virtual sensing. *Applied Stochastic Models in Business and Industry*, *38*(5), 806–829. https://doi.org/10.1002/asmb.2697

Li, S., Griffith, D. A., & Shu, H. (2020). Temperature prediction based on a space–time regression-kriging model. *Journal of Applied Statistics*, *47*(7), 1168–1190. https://doi.org/10.1080/02664763.2019.1671962

Medeiros, E. S. D., De Lima, R. R., Olinda, R. A. D., Dantas, L. G., & Santos, C. A. C. D. (2019). Space–Time Kriging of Precipitation: Modeling the Large-Scale Variation with Model GAMLSS. *Water*, *11*(11), 2368. https://doi.org/10.3390/w11112368

O'Rourke, S., & Kelly, G. E. (2015). Spatio-temporal Modelling of Forest Growth Spanning 50 Years – The Effects of Different Thinning Strategies. *Procedia Environmental Sciences*, *26*, 101–104. https://doi.org/10.1016/j.proenv.2015.05.008

Osman, A. I., Chen, L., Yang, M., Msigwa, G., Farghali, M., Fawzy, S., Rooney, D. W., & Yap, P.-S. (2023). Cost, environmental impact, and resilience of renewable energy under a changing climate: A review. *Environmental Chemistry Letters*, *21*(2), 741–764. https://doi.org/10.1007/s10311-022-01532-8

Pambudi, N. A., Firdaus, R. A., Rizkiana, R., Ulfa, D. K., Salsabila, M. S., Suharno, & Sukatiman. (2023). Renewable Energy in Indonesia: Current Status, Potential, and Future Development. *Sustainability*, *15*(3), 2342. https://doi.org/10.3390/su15032342

Rahmawati, N. (2020). Space-time variogram for daily rainfall estimates using rain gauges and satellite data in mountainous tropical Island of Bali, Indonesia (Preliminary Study). *Journal of Hydrology*, *590*, 125177. https://doi.org/10.1016/j.jhydrol.2020.125177

Sadiq, L. S., Hashim, Z., & Osman, M. (2019). The Impact of Heat on Health and Productivity among Maize Farmers in a Tropical Climate Area. *Journal of Environmental and Public Health*, *2019*(1), 1–7. https://doi.org/10.1155/2019/9896410

Van Zoest, V., Osei, F. B., Hoek, G., & Stein, A. (2020). Spatio-temporal regression kriging for modelling urban $NO_2$ concentrations. *International Journal of Geographical Information Science*, *34*(5), 851–865. https://doi.org/10.1080/13658816.2019.1667501

Yuan, X., Li, S., Chen, J., Yu, H., Yang, T., Wang, C., Huang, S., Chen, H., & Ao, X. (2024). Impacts of Global Climate Change on Agricultural Production: A Comprehensive Review. *Agronomy*, *14*(7), 1360. https://doi.org/10.3390/agronomy14071360

Zateroglu, M. T. (2021). Evaluating The Sunshine Duration Characteristics In Association With Other Climate Variables. *European Journal of Science and Technology*, *Avrupa Bilim Ve Teknoloji Dergisi*(29), 200–207. https://doi.org/10.31590/ejosat.1022639

Zhao, J., Li, C., Yang, T., Tang, Y., Yin, Y., Luan, X., & Sun, S. (2020). Estimation of high spatiotemporal resolution actual evapotranspiration by combining the SWH model with the METRIC model. *Journal of Hydrology*, *586*, 124883. https://doi.org/10.1016/j.jhydrol.2020.124883